

Fraction-dependent variations in cooling efficiency of urban trees across global cities

Wenfeng Zhan^{a,b,c}, Chunli Wang^{a,*}, Shasha Wang^a, Long Li^a, Yingying Ji^a, Huilin Du^a, Fan Huang^a, Sida Jiang^a, Zihan Liu^a, Huyan Fu^d

^a Jiangsu Provincial Key Laboratory of Geographic Information Science and Technology, International Institute for Earth System Science, Nanjing University, Nanjing, Jiangsu 210023, China

^b Jiangsu Center for Collaborative Innovation in Geographical Information Resource Development and Application, Nanjing 210023, China

^c Frontiers Science Center for Critical Earth Material Cycling, Nanjing University, China

^d Department of Geographic Information Science, School of Earth Sciences, Yunnan University, Kunming 650091, Yunnan, China



ARTICLE INFO

Keywords:

Cooling efficiency
Cooling potential
Urban trees
Tree cover percentage
Population heat exposure

ABSTRACT

Investigating the relationship between cooling efficiency (CE) and tree cover percentage (TCP) is critical for planning of green space within cities. However, the spatiotemporal complexities of the intra-city CE-TCP relationship worldwide with distinct climates, as well as the differing impacts of consistently increasing tree cover within urban regions on cooling potential, remain unclear. Here we used satellite-derived MODIS observations to investigate the CE-TCP relationship across 440 global cities during summertime from 2018 to 2020. We further investigated the impacts of enhancing tree cover by a consistent amount in different urban locales on the reduction of population heat exposure among specific age groups. Our results demonstrate a nonlinear CE-TCP relationship globally – CE exhibits an initial sharp decline followed by a gradual reduction as TCP rises, and this nonlinearity is more pronounced in tropical and arid climates than in other climate zones. We observe that 91.4% of cities experience a greater reduction in population heat exposure when introducing the same amount of TCP in areas with fewer trees than in those with denser canopies; and heat exposure mitigation is more prominent for laborers than for vulnerable groups. These insights are critical for developing strategies to minimize urban heat-related health risks.

1. Introduction

Over half of the world's population resides in urban areas (UN, 2022). The confluence of urban expansion and climate change has resulted in augmented and persistent heat exposure among urban residents (Meehl & Tebaldi, 2004; Oke et al., 2017; Wang et al., 2019b; Mitchell, 2021), significantly increasing the likelihood of heat-related illnesses and mortality (Mora et al., 2017; Raymond et al., 2020). Urban greening emerges as an effective solution to minimize heat-related hazards within cities (Bowler et al., 2010; Santamouris, 2014; Alkama and Cescatti, 2016). Among various urban greening

infrastructures, urban trees have superior cooling capacity compared to other vegetation types such as shrubs and grasslands (Schwaab et al., 2021), and their cooling efficiency (CE, usually measured by the change in land surface temperature per 1 % rise in tree cover percentage) have received the most widespread attention (Konarska et al., 2016; Jiao et al., 2017; Leng et al., 2024).

Previous studies have identified significant CE differences across regional or global cities, ranging from 0.07 K/% to 0.45 K/% (Jenerette et al., 2016; Zhou et al., 2017; Wang et al., 2020; Yang et al., 2022; Zhao et al., 2023; Leng et al., 2024). Cities located in arid climates tend to exhibit higher average CE values than those in humid regions (Cheng

Abbreviations: ω_d , extra impact of increased TCP on cooling efficiency; ΔQ , differences in the reduction of population heat exposure between regions with sparse tree cover and denser foliage; CE, cooling efficiency; CE_{ob} , observed CE of each city; CE_{st} , maximum potential CE of each city; $d\beta$, change in tree cover percentage; $dLST$, variation of land surface temperature; LST, land surface temperature; LST_{dt} , average LST of the city in regions with denser foliage; LST_{st} , average LST of the city in regions with relatively sparse tree cover; pop_{dt} , population in areas with denser foliage; pop_{st} , population in areas with relatively sparse tree cover; Q_{dt} , cooling potential in areas with denser foliage; Q_{st} , cooling potential in areas with relatively sparse tree cover; TCP, tree cover percentage.

* Corresponding author at: Nanjing University at Xianlin Campus, No. 163 Xianlin Avenue, Qixia District, Nanjing, Jiangsu 210023, PR China.

E-mail address: chunliwaiyi@foxmail.com (C. Wang).

<https://doi.org/10.1016/j.isprsjprs.2024.07.026>

Received 17 December 2023; Received in revised form 25 July 2024; Accepted 26 July 2024

Available online 9 August 2024

0924-2716/© 2024 International Society for Photogrammetry and Remote Sensing, Inc. (ISPRS). Published by Elsevier B.V. All rights are reserved, including those for text and data mining, AI training, and similar technologies.

et al., 2022; Yang et al., 2022; Cheng et al., 2023). Regarding the spatial scale at which the CE-tree cover percentage (TCP) relationship is investigated, previous studies can be broadly classified into three categories. The first category of studies considers the entire city as a unified single entity without considering the spatial heterogeneity of the CE-TCP relationship within cities, either on regional or global scales (Yang et al., 2022; Du et al., 2024). The second category partitions cities into several regions according to TCP intervals and then examines the CE variations in these partitioned TCP intervals (Zhao et al., 2023). Nevertheless, their involved intervals remain relatively limited (i.e., only spanning from 0 % to 30 %), leading to the difficulties in characterizing the complete continuous dynamics of CE-TCP relationship when TCP changes from zero to a large coverage (i.e., 60 %). The third category captures the continuous curve of the CE-TCP relationship by segmenting the entire city into sufficient TCP intervals (Jenerette et al., 2016; Zhou et al., 2017; Wang et al., 2020). However, such studies are mostly restricted over individual or regional cities.

Regarding the type and form of the CE-TCP relationship, studies indicate that the CE-TCP relationship is complex across distinct cities – a portion of studies propose a constant CE-TCP relationship, i.e., CE remains unchanged with increasing TCP (Hamada & Ohta, 2010; Myint et al., 2013), while others demonstrate a linear or nonlinear one (Zhou et al., 2021; Wang et al., 2022a; Leng et al., 2024). In particular, a few studies propose a linear CE-TCP relationship, such as over Hong Kong in China and Massachusetts in United States (Rogan et al., 2013; Zhou et al., 2021). In contrast, the majority of studies suggest a nonlinear CE-TCP relationship (i.e., cities in North America and China), with CE exhibiting an initial sharp decline followed by a slower decline until it reaches a certain threshold as TCP increases (Wang et al., 2022a; Leng et al., 2024). The inconsistencies in the type and form of the CE-TCP relationship may stem from the differences in urban characteristics and background climate (Bowler et al., 2010; Cheng et al., 2023).

Based on the derived CE-TCP relationship, previous studies examined the effect of uniformly increasing tree cover on the cooling potential among urban residents across global cities (Sinha et al., 2021; Jungman et al., 2023; Massaro et al., 2023). Their results indicate that increasing TCP can effectively reduce population heat exposure and alleviate heat-related health hazards (Sinha et al., 2021; Jungman et al., 2023). A 10 % increase in TCP globally is associated with an approximate 7 % decrease in heat exposure for urban dwellers (Massaro et al., 2023). Such magnitude of reduction in population heat exposure is closely related to the proportion of tree cover – a larger amount in TCP may offer greater cooling potential (Sinha et al., 2021; Jungman et al., 2023; Massaro et al., 2023). The cooling potential for urban dwellers also significantly depends on the population density, age structure, and tree cover percentage of different urban regions (Chakraborty et al., 2019; Hsu et al., 2021; Tuholske et al., 2021; Luo and Lau, 2021; Yin et al., 2023). Hence, investigating the impact of enhancing tree cover by a consistent amount in different urban locales on the cooling potential among specific age groups is crucial for developing strategies to minimize heat-related health risks within cities.

Despite the great progress made regarding the CE-TCP relationship, three issues still persist. First, previous studies either treated the entire city as a single entity or limited their scope to regional cities. This leaves a gap in understanding the spatiotemporal complexities in the CE-TCP relationship, especially from an intra-city perspective globally. Second, there remains incomplete in the understanding of the piecewise impact of external factors on CE (i.e., the extra impact of increasing TCP on CE), especially on how this impact varies from entire absence to large coverage of canopies. Third, the diverse impacts of evenly increasing the same TCP on cooling benefits among specific age groups remain largely unknown within cities worldwide. To address these knowledge gaps, here we investigated the summertime CE-TCP relationship across 440 cities worldwide, using MODIS LST and TCP data (2018–2020). We then examined the impacts of consistently increasing TCP in different urban locales on the reduction of population heat exposure for urban

residents. We consider this study is critical for better developing strategies to minimize health hazards and maximize advantages of trees within urban surroundings.

2. Study area and data

We selected 440 cities worldwide to investigate the complete CE-TCP curve during summer daytime (Fig. 1; more details of city selection are provided in [Section 3.1](#) and [Note S1](#) in [Supporting Information](#)). Both MODIS and auxiliary data were employed in this study. The MODIS data comprise the daily land surface temperature (LST) data, yearly tree cover percentage (TCP) data during 2018–2020, and land cover data for 2018. The daily LST observations from the Terra/Aqua MODIS products (MOD11A1, MYD11A1; 1 km) and the yearly TCP data from the MODIS vegetation continuous fields product (MOD44B, 250 m) were both used to calculate the cooling efficiency (CE) in various TCP ranges across global cities. The MODIS land cover product (MCD12Q1, 500 m) defined by the International Geosphere-Biosphere Programme (IGBP) classification framework were used to eliminate the influence of special pixels (i.e., permanent wetlands, water bodies, snow, and glaciers) on the calculation of CE (Yang et al., 2022). Note that further details on preprocessing of these data are provided in [Note S1](#) in [Supplementary Information](#).

The auxiliary data mainly consist of global urban boundary (GUB) data for 2018, the national population data for 2019, and elevation data. The GUB data were used to identify the scope of urban area worldwide, which can be accessed at a public information-sharing center (<http://data.ess.tsinghua.edu.cn>). The GUB data were generated from the global artificial impervious area (GAIA) products and exhibit a higher degree of accuracy in comparison to similar products (Li et al., 2020). The national population data with different age structures (0–14 years old, 15–64 years old and over 65 years old) were used to examine the impacts of uniformly enhancing TCP within different urban regions on cooling potential for age-specific groups, which can be obtained from United States statistics (UN, 2022). More explanations and sensitivity analysis for using national population data with different age structures are provided in [Figures S1 & S2](#) and [Note S2](#) in [Supplementary Information](#). The elevation data (GOTOPO30, approximately 1 km) were employed to eliminate the pixels with elevations exceeding ±50 m from the urban median elevation to avoid the influence of terrain on the urban LST (Wang et al., 2023). All of the aforementioned data were resampled to 250 m using the nearest neighbor method.

3. Materials and methods

3.1. Selection and delineation of global cities

A total of 440 cities worldwide were selected according to two criteria. First, cities with an urban area larger than 50 km² in 2018 according to the GUB data were chosen. Second, cities with a TCP range of 0 % to 60 % were selected. The TCP range of 0 % to 60 % instead of 0 % to 100 % was selected mainly owing to the limited number of pixels when TCP surpasses 60 %. Note that the criterion of TCP range for cities in Africa and India was adjusted to only include cities with TCP values from 0 % to 30 % due to the lack of pixels with TCP values exceeding 30 % for these cities. Consequently, a total of 54 African cities and 26 Indian cities were ultimately selected to ensure a broad representation of global cities in such regions. Our closer sensitivity analysis shows a minimal impact of the uneven distribution of global cities on the principal findings (see [Figure S3](#) and [Note S3](#) in [Supporting Information](#)).

Our study primarily focused on the CE-TCP relationship across different urban regions of each city due to the discrepancies of population density and heat-related health risk in these regions (Chakraborty et al., 2019). Therefore, we further divided each selected city into 12 TCP bins with an interval of 5 % (i.e., 0 %–5 %, 5 %–10 %, 10 %–15 %, 15 %–20 %, 20 %–25 %, 25 %–30 %, 30 %–35 % and so on) to

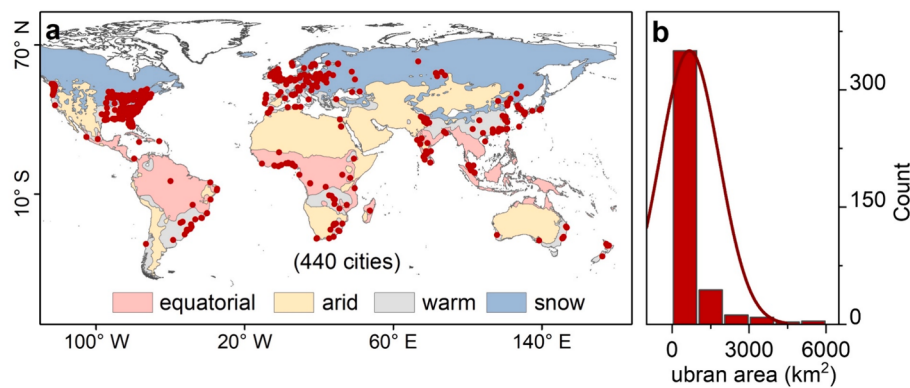


Fig. 1. Geographical distribution of 440 cities worldwide (a); and the frequency of city size for global cities (b).

investigate a complete continuous CE-TCP curve from zero to extensive coverage (i.e., 60 %). To ensure the precision of CE calculations across global cities, all TCP bins within each city were set to contain a minimum of eight pixels (Liu et al., 2024). Our further sensitivity analysis also shows that the TCP interval of 5 % exerts a negligible influence on the spatial pattern of CE and the CE-TCP relationship (refer to Figure S4 and Note S4 in Supporting Information).

3.2. Quantification of CE and investigation into CE-TCP relationship

3.2.1. Quantification of cooling efficiency

The cooling efficiency (CE) has been extensively used to quantify the cooling capacity of urban trees (Yang et al., 2022; Cheng et al., 2023). In this study, CE of each city was calculated by the magnitude of change in LST for a 1 % increase in tree cover percentage (denoted by β), i.e., the negative slope between LST and TCP (Eq. (1); Wang et al., 2019a; Zhao et al., 2023).

$$\text{CE} = -\frac{d\text{LST}}{d\beta} \quad (1)$$

where CE denotes the cooling efficiency of each city; and $d\text{LST}$ and $d\beta$ represent the change in LST and TCP, respectively. A positive CE value ($\text{CE} > 0$) indicates a decreasing LST as TCP rises, with a higher value denoting a greater cooling efficiency. Conversely, a negative CE value ($\text{CE} < 0$) indicates an enhanced LST as TCP rises. The negative correlation between the LST and TCP implies that the LST decreases as TCP increases, yet the corresponding cooling ability of trees is positive. It is thus understandable to multiply the slope by -1 to align the magnitude of the slope with the cooling capacity (Wang et al., 2020; Zhou et al., 2021).

3.2.2. Investigation into spatiotemporal complexities of CE-TCP relationship

Our study mainly focused on the spatiotemporal patterns of CE-TCP relationship during summer daytime, with more explanations for the season selection provided in Note S5 in Supporting Information. To characterize the CE-TCP relationship in summer, we first calculated the mean monthly daytime CE within each TCP bin for each city worldwide, and then obtained the mean summer CE within each TCP bin of each city from 2018 to 2020. Before the CE calculation, we eliminated the pixels labelled as permanent wetland, water body, glacier or snow, and pixels with elevations exceeding ± 50 m of the urban median elevation to minimize the effect of water bodies and terrain on the LST/CE (Yang et al., 2022; Wang et al., 2023). Regarding the spatiotemporal analysis, we investigated the global CE variations within the sufficient urban regions as well as the spatial pattern of CE in regions with relatively low TCP ($\beta < 50\%$) and high TCP ($\beta \geq 50\%$; see Figure S5 for more information on delineation of low and high TCP regions). We also

aggregated all cities into each climate and continent to investigate the CE-TCP relationship across climates and continents in summer (Section 4.1). Note that results regarding the CE-TCP relationship for the other three seasons are provided in Figures S6 to S8 in Supporting Information.

3.3. Conceptual framework on the CE-TCP relationship

To clarify the potential effects of increasing TCP on CE, we proposed a conceptual framework for analyzing the CE-TCP relationship (Fig. 2). The decrease of LST is generally linear as TCP rises under ideal situations, suggesting a theoretical zero-impact of external factors on LST/CE (Rogan et al., 2013; Zhou et al., 2021), as depicted by the shaded area between the purple and blue lines in Fig. 2a. However, the relationship between TCP and LST/CE may not be entirely consistent with the zero-impact hypothesis in realistic settings, suggesting the existence of additional impact induced by various environmental factors. For example, external factors such as background climate may contribute to elevated air humidity as TCP rises, which can reduce the vapor pressure deficit (VPD) between leaf stomata and the air, ultimately resulting in a decrease in leaf transpiration rate (Wang et al., 2020). These external factors may in turn exert effects on LST/CE, i.e., the extra effect of TCP on LST/CE, represented by the shaded area between the red and purple lines as shown in Fig. 2. Therefore, a non-linear relationship between LST/CE and TCP would be anticipated if more external factors are considered (Li et al., 2015; Yu et al., 2018; Lambers and Oliveira, 2019; Wang et al., 2019a).

The theoretical zero-impact line ($\omega = 0$), also known as the constant cooling efficiency line or maximum potential cooling efficiency line, is defined as the tangent line of the LST observation curve when TCP is less than 5 % (represented by the purple line in Fig. 2). This zero-impact line represents the CE-TCP relationship under ideal conditions, without considering the impact of external factors. The extra impact (ω_d) refers to the additional promotion or inhibition effect of external factors on CE as trees transition from being sparse to dense (Eq. (2) & Fig. 2b).

$$\omega_d = \frac{\text{CE}_{\text{obs}} - \text{CE}_{\text{st}}}{\text{CE}_{\text{st}}} \quad (2)$$

where ω_d denotes the extra impact of increased TCP on CE; and CE_{ob} and CE_{st} represent the observed CE and the maximum potential CE for each city worldwide, respectively. A positive ω_d ($\omega_d > 0$) denotes a promoting effect of external factors on CE; otherwise, it represents an inhibiting effect on CE.

3.4. Impacts of uniformly enhancing tree cover within different urban regions on cooling potential for specific age groups

There are significant disparities in cooling potential among specific age groups due to variations in LST and population within intra-city

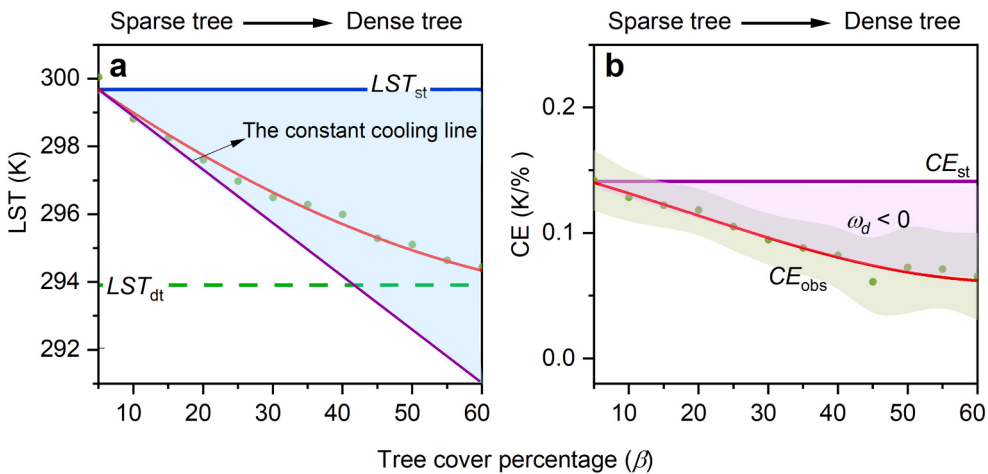


Fig. 2. Conceptual framework of LST (a) and CE (b) with varying tree cover percentage (TCP) for each city. LST_{st} and LST_{dt} refer to the average LST of the city in regions with relatively sparse tree cover ($\beta < 5\%$) and denser foliage ($55\% \leq \beta < 60\%$); and CE_{st} and CE_{obs} denote the maximum potential CE and the observed CE of each city, respectively.

regions (Massaro et al., 2023). To reveal the impacts of enhancing tree cover by a consistent amount in urban regions on the cooling potential among urban residents, we investigated the differences in the reduction of heat exposure (ΔQ) between regions with sparse tree cover and denser foliage from global, climatic, and continental perspectives.

Despite the existence of numerous metrics designed to quantify the population heat exposure, there is currently no universally agreed-upon criterion (Biardeau et al., 2020; Zhao et al., 2021). This study employed a widely accepted and straightforward method to assess the population heat exposure, quantified by multiplying the surface temperature by urban populations within a given area (Laaidi et al., 2012; Yuan et al., 2022).

3.4.1. Quantification of the impacts of evenly increasing tree cover within urban regions on cooling potential for age-specific groups

The disparity in cooling potential (i.e., the amount of population heat exposure reduction) within different urban regions (ΔQ) was quantified as the difference in cooling potential between low TCP regions ($\beta < 20\%$) and relatively high TCP regions ($30\% \leq \beta < 50\%$; Eq. (3)). For the low TCP regions, the cooling potential was quantified as the discrepancies in the population heat exposure between sparse zone-1 ($\beta < 10\%$) and sparse zone-2 ($10\% \leq \beta < 20\%$, with a 10% increase in TCP based on zone-1; Eq. (4)). For the relatively high TCP regions, the cooling potential was quantified as the difference in the population heat exposure between dense zone-3 ($30\% \leq \beta < 40\%$) and dense zone-4 ($40\% \leq \beta < 50\%$, with a 10% TCP increase based on zone-3; Eq. (5)). Note that areas with TCP exceeding 50% were excluded from the analysis because minimal fluctuations in CE and population would lead to negligible alterations in population heat exposure (Zhou et al., 2017; Cheng et al., 2022).

$$\Delta Q = Q_{st} - Q_{dt} \quad (3)$$

$$Q_{st} = pop_{st} \times (LST_{zone-1} - LST_{zone-2}) \quad (4)$$

$$Q_{dt} = pop_{dt} \times (LST_{zone-3} - LST_{zone-4}) \quad (5)$$

where Q_{st} and Q_{dt} represent the cooling potential in areas with relatively sparse tree cover and denser foliage, respectively; LST_{zone-1} , LST_{zone-2} , LST_{zone-3} , and LST_{zone-4} are the average surface temperature in zone-1, zone-2, zone-3, and zone-4, respectively; and pop_{st} and pop_{dt} denote the population in regions with low TCP and relatively high TCP, respectively.

3.4.2. Investigation of the impacts of enhancing the consistent TCP in urban locales on cooling potential among specific age groups

To assess the potential effects of enhancing TCP by a consistent amount within different urban regions on mitigated heat exposure for specific age groups, we first calculated the urban population with varying age structures in areas with fewer trees and denser foliage based on the national age-specific population data. Subsequently, we investigated the difference in mitigated heat exposure (ΔQ) among specific age groups when deploying the constant tree cover in those urban regions (see Eqs. (3)–(5)). Finally, we analyzed the consequences of ΔQ across climates and continents for different social groups (Section 4.3). The social groups were categorized as labor (i.e., populations aged 15–64 years) and vulnerable groups (i.e., populations aged 0–14 years and >65 years) based on the national age structure data. The national age structure data rather than the city-level data were employed mainly due to their universal applicability in urban thermal environments and inaccessibility for the accurate age-specific population data at the city level worldwide (Park et al., 2020; Falchetta et al., 2024). Further sensitivity analysis of the national age-specific population shows that the use of these national data would barely affect the main findings, as detailed in Table S1, Figures S1 & S2, and Note S2 in Supporting Information.

4. Results

4.1. Spatiotemporal patterns of the CE-TCP relationship across global cities

Globally, our results show that CE exhibits an initial sharp decline followed by a gradual decrease as TCP rises, suggesting the higher CE in lower fraction of coverage. This nonlinear relationship is more pronounced in summer than in other seasons (Figures S6 to S8). The global mean CE in summer reaches 0.10 ± 0.05 K%/ (Fig. 3c). The revealed nonlinear CE-TCP relationship worldwide basically aligns with the majority of previous findings focusing on individual or regional cities (Wang et al., 2022a; Leng et al., 2024). However, previous investigation also reported a linear CE-TCP relationship in few cities like Hong Kong and Massachusetts (Rogan et al., 2013; Zhou et al., 2021). Such different patterns may be attributed to the discrepancies in geographical location and background climate. In particular, we also observed a similar nonlinear relationship between evapotranspiration rate and leaf area index that helps consolidate these findings (refer to Figure S9 and Note S5 in Supplementary Information for details).

The CE significantly differs within urban regions worldwide. For

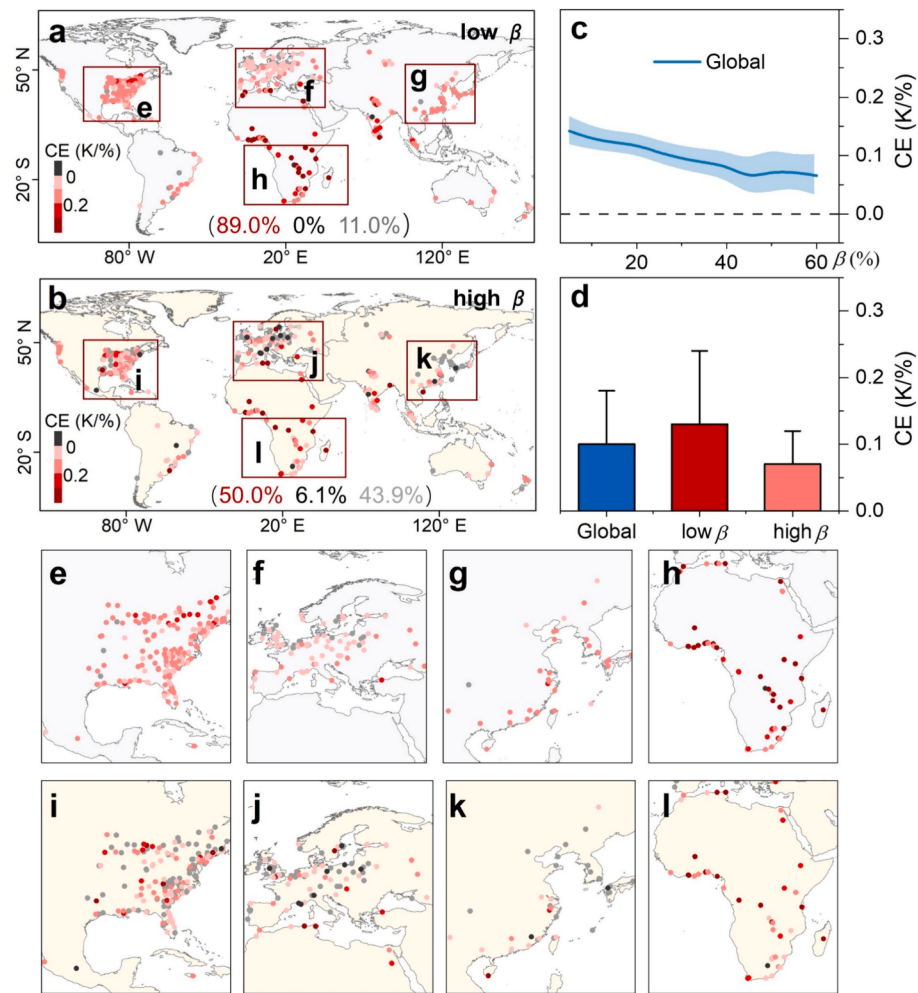


Fig. 3. Global pattern of CE among different TCP regions during summer daytime. Spatial distribution of CE in low TCP regions ($\beta < 50\%$; **a**) and in high TCP regions ($\beta \geq 50\%$; **b**); the global CE-TCP relationship (**c**); the mean CE across the globe and different TCP regions (**d**); and the enlarged view of cities in North America, Europe, Asia, and South America in the low (**e-h**) and high (**i-l**) TCP zones. The red, black, and gray dots represent the percentages with a significant positive, significant negative, and insignificant CE, respectively. (For interpretation of the references to colour in this figure legend, the reader is referred to the web version of this article.)

low-TCP regions ($\beta < 50\%$), the global mean CE in summer reaches $0.12 \pm 0.08 \text{ K}/\%$ (**Fig. 3a & d**). The vast majority of cities (i.e., 89 %) exhibit a significantly positive CE (i.e., a decreasing LST as TCP rises), with the larger CEs in cities of Asia, North America, and Africa, while relatively lower values in European cities (**Fig. 3e-h**). For high-TCP regions ($\beta \geq 50\%$), the mean summertime CE reaches $0.07 \pm 0.06 \text{ K}/\%$ (**Fig. 3b & d**). The cities with positive CEs only account for around 50 %. In addition, a portion of individual cities located in lower TCP areas exhibit the significantly positive CEs (i.e., cooling effect), whereas those located in higher TCP areas have the significantly negative CEs (i.e., warming effect), similar to previous results showing that the increase of tree cover does not always lead to a reduction in LST ([Wang et al., 2022b](#); [Cheng et al., 2022](#); [Du et al., 2024](#)). This indicates an enhanced LST as TCP increases in some cities when TCP exceeds 50 %, probably due to the difference in tree species, tree canopy, background climate, local surface properties, and human activities ([Lambers and Oliveira, 2019](#); [Wang et al., 2020](#)).

Regarding climate zones, the mean CE is the highest in arid ($0.12 \pm 0.08 \text{ K}/\%$), followed by equatorial ($0.11 \pm 0.07 \text{ K}/\%$), snow ($0.10 \pm 0.06 \text{ K}/\%$) and temperate ($0.09 \pm 0.05 \text{ K}/\%$) zones (**Fig. 4c**). This pattern is generally consistent with previous findings based on case studies (e.g., cities in southern California), suggesting a higher CE in dry and hot desert regions ([Tayyebi & Jenerette 2016](#); [Yu et al., 2018](#); [Cheng et al., 2023](#)).

The variation magnitude of the CE-TCP relationship, denoted as the difference between the highest CE and lowest CE, also reaches the largest in equatorial ($0.20 \text{ K}/\%$), followed by in arid climates ($0.16 \text{ K}/\%$), temperate ($0.10 \text{ K}/\%$), and snow climates ($0.11 \text{ K}/\%$). The larger CE-TCP variation in equatorial zone may be due to the higher transpiration rates caused by the higher temperatures and relative humidity, finally resulting in a larger CE variation as TCP rises over these regions ([Swann et al., 2012](#); [Aparecido et al., 2016](#)).

When considering continents, Asia ($0.11 \pm 0.03 \text{ K}/\%$) and North America ($0.11 \pm 0.02 \text{ K}/\%$) possess the higher CEs, followed by Africa ($0.09 \pm 0.01 \text{ K}/\%$), and the CE is relatively lower in South America, Oceania, and Europe (**Fig. 4d**). A higher average CE was also reported in North American cities ([Zhao et al., 2023](#)). In terms of the CE variation with TCP, cities in South America show the highest variation of CE ($0.22 \text{ K}/\%$), followed by Asia ($0.20 \text{ K}/\%$), and Africa ($0.19 \text{ K}/\%$). In contrast, such variation is less prominent in Oceania ($0.14 \text{ K}/\%$), North America ($0.10 \text{ K}/\%$), and Europe ($0.06 \text{ K}/\%$) (**Fig. 4b**). Note that our findings provide a more comprehensive understanding of the CE-TCP relationship globally from the intra-city scale compared to previous studies that either treated the city as a single entity or limited their scope to regional cities ([Myint et al., 2013](#); [Zhou et al., 2021](#)).

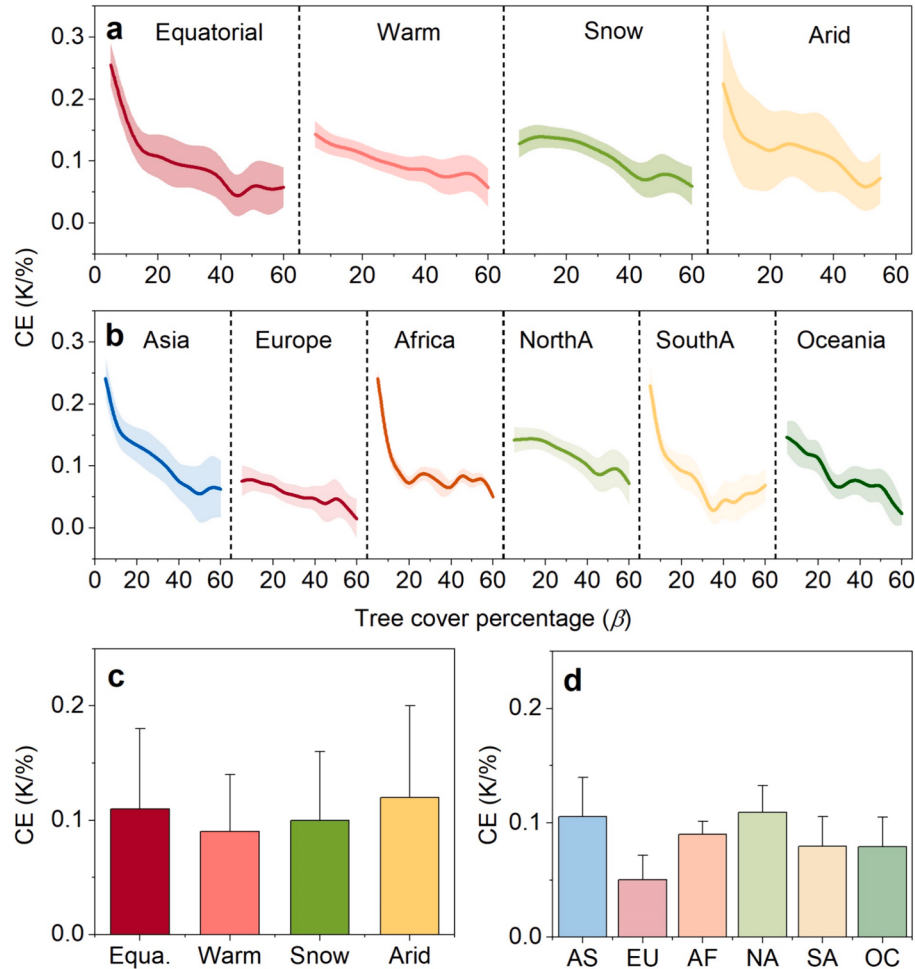


Fig. 4. Average CE and its variation with TCP across climates and continents during summer daytime. The CE-TCP relationship in different climates (a) and continents (b); and the mean summertime CE in climates (c) and continents (d). AS, EU, AF, NA, SA, and OC are abbreviations for Asia, Europe, Africa, North America, South America, and Oceania, respectively.

4.2. Underlying impacts of external factors on CE as TCP rises

We evaluated the underlying impacts of external factors on CE as TCP rises (denoted by ω_d) worldwide (Fig. 5). The results show that the global average ω_d is -38.7% in summer, suggesting a hindering effect of external factors on CE. The results also demonstrate a decrease in ω_d with increasing TCP, indicating an increasing hindering effect of external factors on CE as TCP increases (Fig. 5c). There are large discrepancies in average value and spatial pattern of ω_d within different urban regions (Fig. 5). In the low-TCP regions, the global mean ω_d is -28.97% . Among them, cities with a significantly negative ω_d (i.e., a hindering effect of external factors on CE) account for 49.2 %, while cities with a significantly positive ω_d (i.e., a promoting effect on CE) account for 13.2 % (Fig. 5a). For the high-TCP regions, the average inhibition effect is generally higher (-48.35%) than in low-TCP regions (Fig. 5d). Around 36.3 % of cities exhibit a significantly negative ω_d , while 12.1 % of cities show a significantly positive ω_d (Fig. 5b). In both low and high TCP regions, a portion of cities in North America and Europe consistently show a significantly positive ω_d (i.e., promoting effect; see Fig. 5e & f, Fig. 5i & j). This phenomenon may be attributed to their lower CEs, and influences of background climate (Lambers and Oliveira, 2019; Wang & Zhou, 2022).

The average ω_d and its variation along with TCP across climates and continents are provided in Fig. 6. Typically, there is a nonlinear relationship between ω_d and TCP across regions, demonstrating a gradual decrease in ω_d as TCP increases (Fig. 6a & b). The strongest effect is

observed in equatorial zone (-56.5%), followed by the arid zone (-36.3%), snow (-32.5%), and warm zone (-29.4% ; Fig. 6c). The larger effect in equatorial and arid zones reflects a stronger hindering effect of external factors on CE due to larger CEs in those regions (Yu et al., 2018). In terms of continents, the hindering effect is the strongest in Africa (-66.4%), followed by South America (-62.0%), Asia (-54.8%), and Europe (-46.1%). By comparison, the effect is relatively weaker in North America (-15.4%) and Oceania (-8.8% ; Fig. 6d). In particular, there are stronger inhibitory effects in China (-60.7%), India (-57.7%), and Brazil (-60.4%) than in other countries (Figure S10). Compared to previous studies only focusing on the CE-TCP relationship (Myint et al., 2013; Wang et al., 2022a), our findings demonstrate a substantial inhibitory effect of external factors on CE as TCP rise, and they prove the nonlinearity of the CE-TCP relationship globally.

4.3. Effects of increasing TCP within regions on urban heat exposure

We examined the impacts of uniformly increasing tree cover (i.e., 10 %) within urban regions with varying TCP on the cooling potential for age-specific groups (ΔQ) (Fig. 7). The results show that the global total ΔQ is approximately 2.3×10^7 persons-K, indicating that the trees planted in lower coverage tend to have a greater cooling potential than those in denser foliage (Figure S11). The labor groups benefit more from this mitigation, with reduced heat exposure reaching 1.5×10^7 persons-K, while the vulnerable groups reaching 0.8×10^7 persons-K.

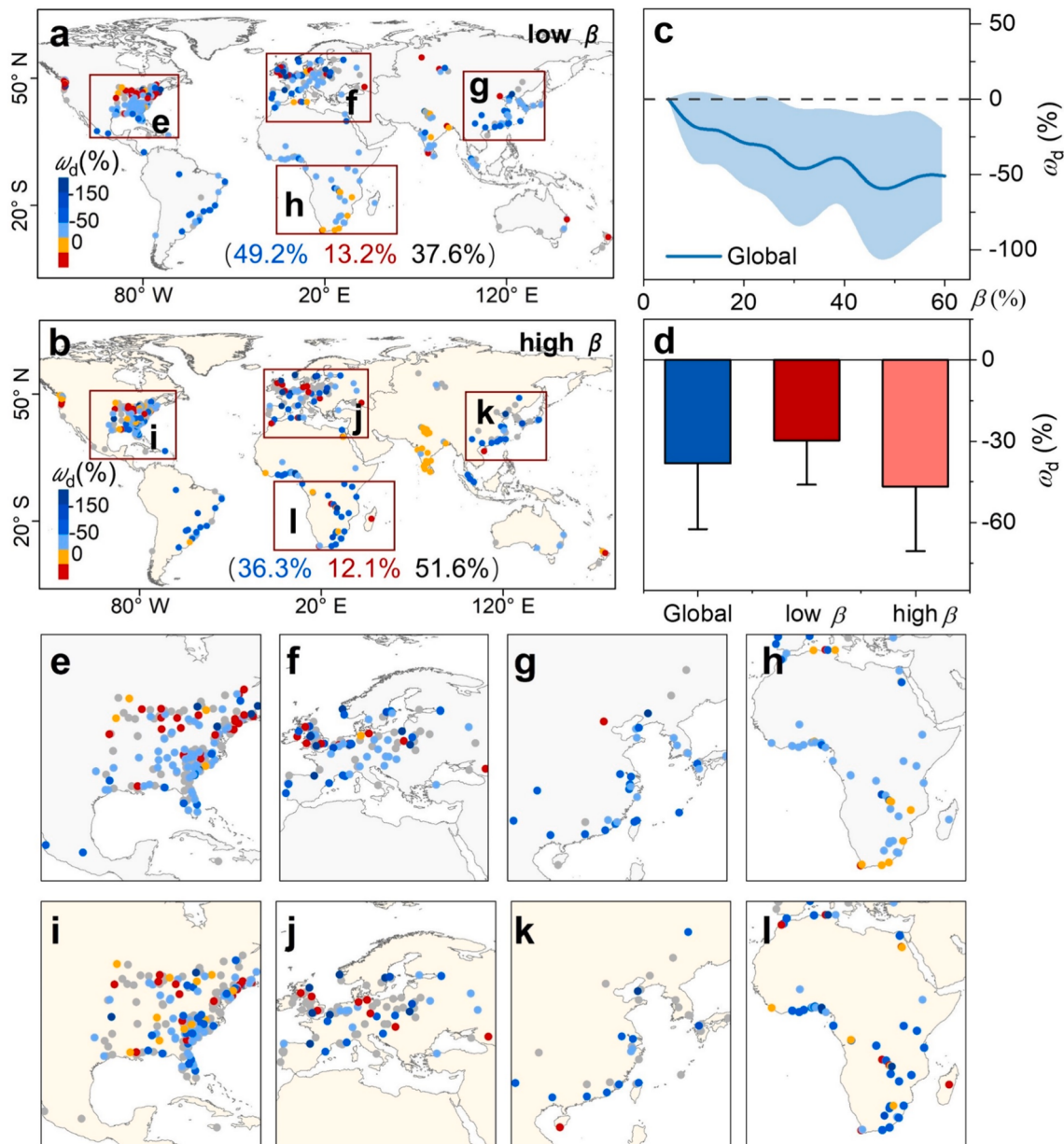


Fig. 5. Spatial pattern on the impact of external factors on CE (denoted as ω_d) worldwide and its variations as TCP rises during summer daytime. Spatial pattern of ω_d in low-TCP ($\beta < 50\%$; a) and high-TCP regions ($\beta \geq 50\%$; b); global variation of ω_d with increased TCP (c); average ω_d across the globe and different TCP regions (d); and enlarged subplots for cities in North America, Europe, Asia, and South America in low-TCP (e-h) and high-TCP regions (i-l). The blue, red and black dots represent the percentage of cities with a significant negative, significant positive, and insignificant ω_d , respectively. A negative ω_d indicates the inhibitory effect of external factors on CE, while a positive one denotes the promoting effect. (For interpretation of the references to colour in this figure legend, the reader is referred to the web version of this article.)

(Fig. 7b). Globally, 93 % of the cities exhibit a stronger cooling potential over low TCP regions (Fig. 7a), while the remaining 7 % of cities (i.e., located in North America) exhibit a stronger cooling potential in regions with denser foliage (Fig. 7c), mainly due to their higher CE variations (Figure S12). Earlier studies only focused on the mitigated heat exposure of the total population in the entire urban regions (Sinha et al., 2021; Jungman et al., 2023; Massaro et al., 2023), yet our results further demonstrate the cooling potential of age-specific groups across different urban regions within cities.

The largest ΔQ occurs in warm zone (1.5×10^7 persons-K), followed by the equatorial (0.4×10^7 persons-K), snow (0.3×10^7 persons-K), and arid zone (0.6×10^6 persons-K; Fig. 8c). A higher ΔQ in the warm zone may be due to a larger population difference between regions with fewer trees and denser foliage (Figure S13). Across continents, the largest ΔQ

is in Asia (1.3×10^7 persons-K), followed by South America (6.2×10^6 persons-K) and Africa (2.3×10^6 persons-K). The ΔQ is relatively low in North America, Europe, and Oceania, indicating less discrepancies in the mitigated heat exposure within regions (Fig. 8d). In terms of the age-specific groups, our results show that the labor and vulnerable groups in Asia and South America consistently display larger heat exposure mitigation in regions with fewer trees than in regions with denser foliage (Fig. 8a & b). However, the mitigated heat exposure is comparable for labor (1.3×10^6 persons-K) and vulnerable groups (1.0×10^6 persons-K) in African cities due to the relatively small discrepancies in the age-specific population within cities (Figure S13). Our results also show that the labor group benefits more from the increasing TCP than the vulnerable group both in sparse and denser foliage regions (Figures S14 & 15). This is slightly different from the case in Baltimore, which

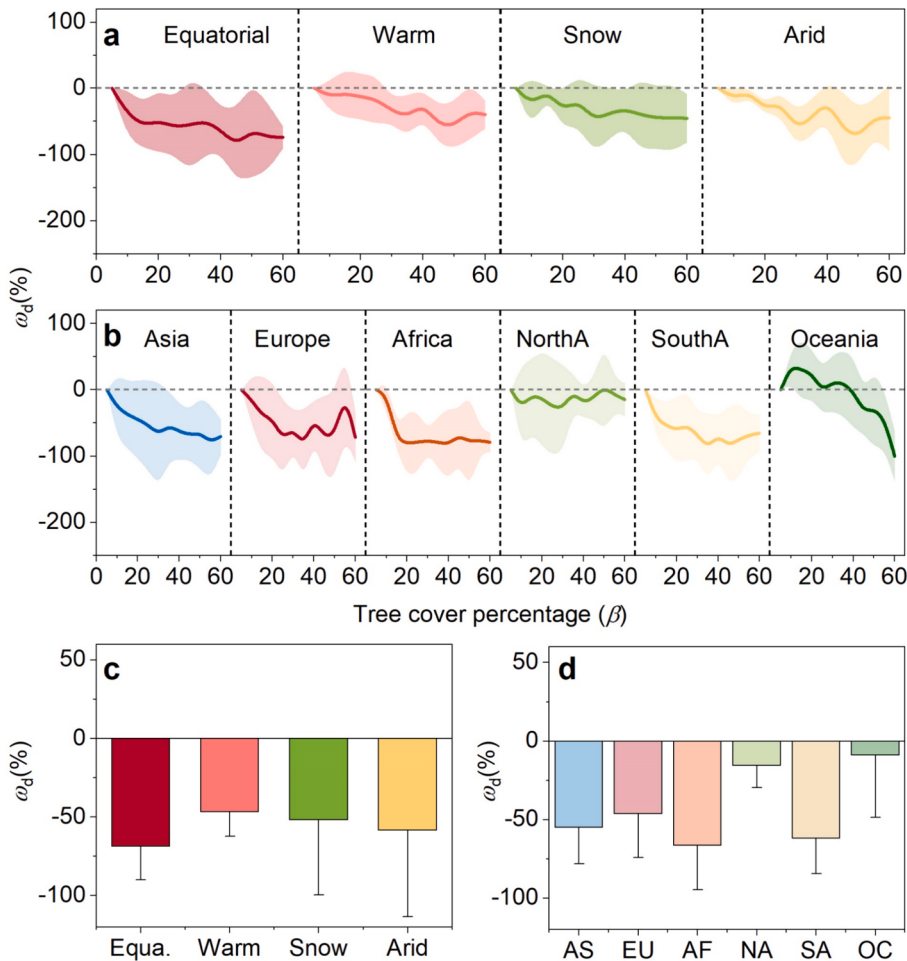


Fig. 6. Average ω_d and its variation along TCP across climates and continents during summer daytime. The variation of ω_d as TCP increases across climates (a) and continents (b); and mean ω_d across climates (c) and continents (d). AS, EU, AF, NA, SA, and OC denote Asia, Europe, Africa, North America, South America, and Oceania, respectively.

reported that increasing TCP reduced more heat exposure for vulnerable than for labor populations (Huang et al., 2011; Sinha et al., 2021).

5. Discussion and implication

5.1. Added values of this current study

Our analysis offers added values into the CE-TCP relationship compared to prior studies. Most previous investigations considered the entire city as a unified entity, neglecting the spatial heterogeneity of CE-TCP relationship within cities worldwide (Yang et al., 2022; Du et al., 2024). A recent pioneering study addressed this by meticulously segmenting cities into several regions based on distinct TCP intervals (Zhao et al., 2023). However, such analysis was constrained by a limited range of TCP intervals (i.e., 0 % to 30 %), which hindered a comprehensive understanding of the continuous dynamics of CE-TCP relationships, particularly as TCP varies from zero to extensive coverage (i.e., 60 %). Although some studies have obtained such continuous dynamics of CE-TCP relationship within cities, these investigations typically focus on individual or regional cities and their obtained conclusions remain often contractionary (i.e., linear or nonlinear CE-TCP relationship) due to differing climatic contexts (Rogan et al., 2013; Zhou et al., 2021; Wang et al., 2022a; Leng et al., 2024). To fill these gaps, our current study utilized a more detailed division strategy for each city with extensive TCP range, and thoroughly examined the intra-city CE-TCP relationship across global cities with diverse climatic contexts. By this way, our

analysis reconciles previous findings and demonstrates a nonlinear CE-TCP relationship from global, climatic, and continental perspective (Fig. 3 & Note S5 in Supporting Information). Our study also suggests an inhibitory effect of external factors on CE as TCP rises (Fig. 5), providing a new support for these nonlinear relationships.

Regarding the cooling potential of urban trees in mitigating urban overheating and associated population heat exposure, an insightful previous investigation has suggested that an increase in TCP by $5.3 \pm 3.8\%$ can reduce LST by $1.5 \pm 1.3\text{ }^{\circ}\text{C}$ worldwide (Zhao et al., 2023). Such a TCP increase can also lower total population heat exposure and heat-related mortality (Sinha et al., 2021; Iungman et al., 2023; Massaro et al., 2023). However, these studies often consider cities as homogeneous units, and focus on the cooling benefits of urban trees for the entire population. The differential impacts of the same TCP increase on heat exposure mitigation across various urban locales and among different age groups remain largely unclear. By contrast, our study analyzed the consequences of consistently increasing TCP within different urban regions on cooling potential for specific age groups. We found that increasing TCP yields a larger reduction of population heat exposure in regions with fewer trees; and the cooling potential is more significant for labors than that for vulnerable populations (Fig. 7).

5.2. Implications and uncertainties

Strategies for mitigating urban heat-related exposure risks should be tailored to local conditions owing to the spatial discrepancies in CE, age

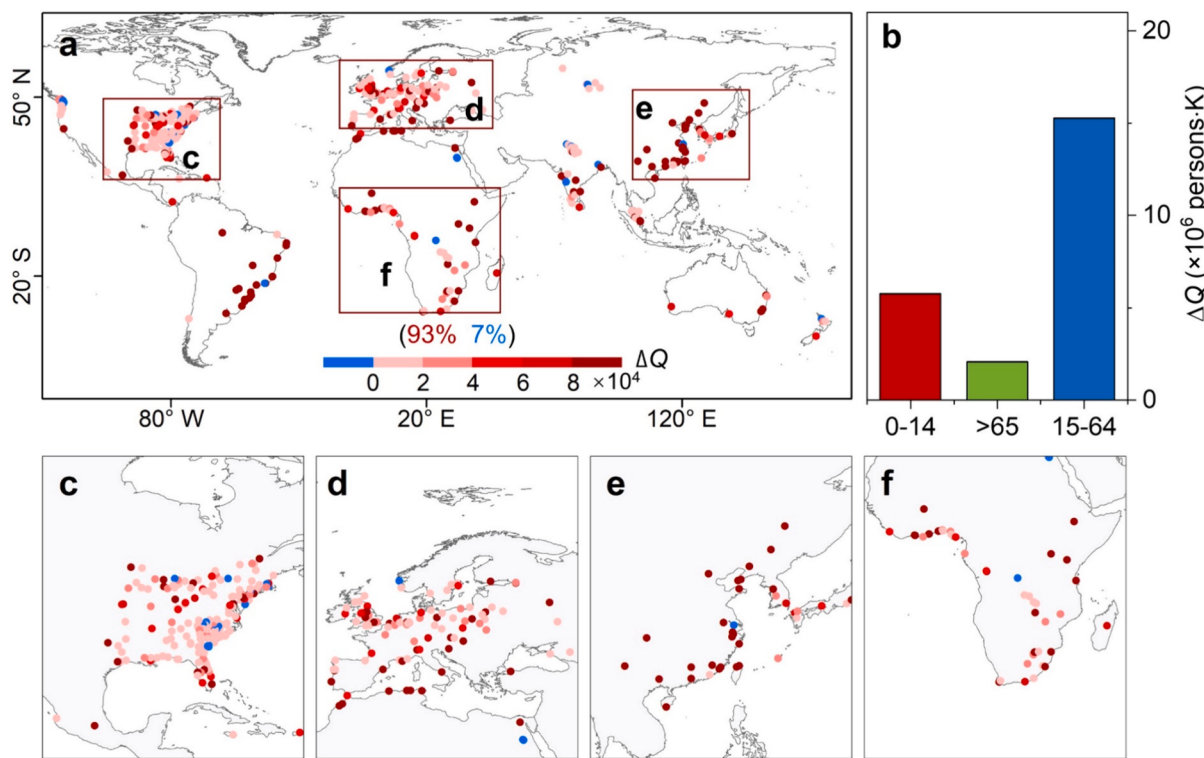


Fig. 7. Global pattern of ΔQ (a) and total ΔQ for different age-specific groups during summer daytime (b). Enlarged subplots for cities in North America (c), Europe (d), Asia (e), and South America cities (f), respectively. The red and blue dots represent the percentages of global cities with positive and negative values in ΔQ , respectively. (For interpretation of the references to colour in this figure legend, the reader is referred to the web version of this article.)

structure of urban population, and population heat exposure within different urban locales. Our results show that for urban regions with sparse tree cover, prioritizing urban greening strategies is a promising strategy to regulate the urban-related exposure risk (Fig. 7a), due to their greater CEs and more intense population heat exposure (Zhou et al., 2021; Yin et al., 2023). Conversely, for urban surfaces with denser foliage (i.e., high TCP), additional tree planting might reduce cooling efficiency (Fig. 5). Therefore, our study cautions that the implementation of specialized cooling materials may be more appropriate for such regions (Fig. 5). For regions with limited resources yet severe heat-related risks (such as Africa), planting trees in right locations and developing applicable warning systems for extreme heat management may be essential (Figure S14a). Our findings also reveal that the cooling potential of uniformly increasing tree cover within regions is more prominent for labor than for vulnerable groups (Fig. 7b), highlighting the significance of designing heat mitigation strategies tailored to specific age groups.

Several limitations warrant consideration in future work. First, we utilized MODIS products instead of Landsat data for CE evaluation, mainly due to the large amounts of missing pixels in Landsat images caused by their long revisit period (16 days), fringe gap, and cloud contamination. However, the relatively coarse resolution (i.e., 1 km) of the MODIS products may be insufficient for the fine-scale evaluation of CE. Second, our assessments were based on land surface temperature (LST) rather than surface air temperature (SAT) data for two main considerations: (1) LST data have been extensively employed to quantify the CE, and they can well reflect the heat exchange between the ground and the surrounding environment (Du et al., 2024; Leng et al., 2024); and (2) SAT data usually lack spatially continuous coverage due to the uneven distribution and limited number of ground-based stations (Anderson et al., 2013; Biardeau et al., 2020). Further research is required to investigate the CE-TCP relationship at a finer spatial scale based on SAT data that is more related to heat stress within cities.

6. Conclusions

This study provides new evidence for the nonlinear CE-TCP relationship within cities worldwide with diverse climatic contexts and offers valuable insights into mitigating population heat exposure in different urban regions. Our research reveals that the global CE is 0.10 ± 0.05 K/% in summer, and as TCP rises, CE exhibits an initial sharp drop, followed by a gradual decline globally. Such nonlinearity is more evident in equatorial (with a variation range of 0.20 K/%) and arid (0.16 K/%) climates compared to snow (0.11 K/%) and temperate (0.10 K/%) zones. The global mean extra impact of increasing TCP on CE is -38.7% , implying an inhibition effect of various factors on CE. Our results further indicate that there is a stronger potential for mitigating heat exposure when deploying equal amounts of TCP in regions with sparse tree coverage compared to those in regions with denser foliage. Specifically, 91.4 % of cities exhibit a greater reduction in population heat exposure when enhancing the same amount of TCP in areas with fewer trees ($TCP < 10\%$) than in those with denser canopies ($30\% \leq TCP < 40\%$). The laborers experience a more significant decrease in heat exposure than vulnerable groups. Our findings advance the understanding of the global CE-TCP relationship within cities, and they provide valuable information for planning urban green space and formulating more appropriate policies to mitigate heat-related risk within cities.

CRediT authorship contribution statement

Wenfeng Zhan: Writing – review & editing, Supervision, Methodology, Funding acquisition, Conceptualization, Formal analysis. **Chunli Wang:** Writing – review & editing, Writing – original draft, Visualization, Validation, Methodology, Formal analysis, Conceptualization, Funding acquisition. **Shasha Wang:** Writing – review & editing, Methodology. **Long Li:** Writing – review & editing. **Yingying Ji:** Writing – review & editing. **Huilin Du:** Writing – review & editing. **Fan Huang:** Writing – review & editing. **Sida Jiang:** Writing – review & editing.

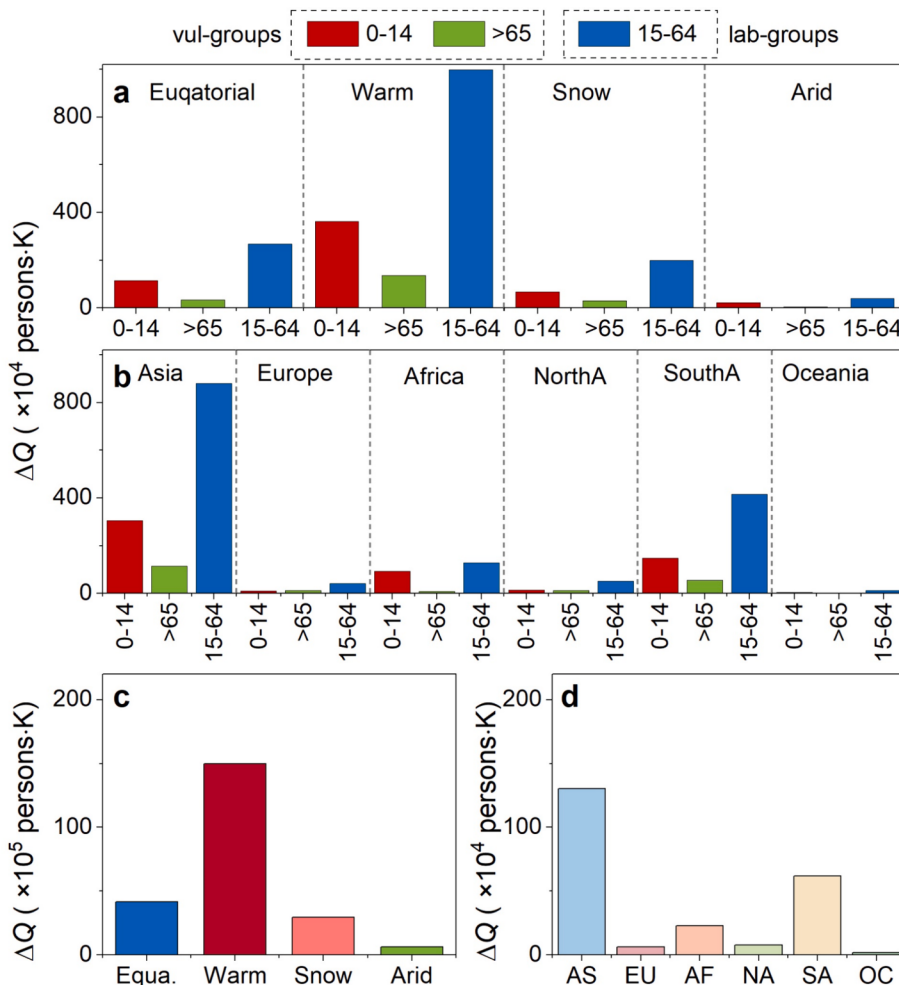


Fig. 8. Total and age-specific ΔQ across climates and continents during summer daytime. The age-specific ΔQ across climates (a) and continents (b); total ΔQ across various climates (c) and continents (d).

Zihan Liu: Writing – review & editing. Huyan Fu: Writing – review & editing, Funding acquisition.

Declaration of competing interest

The authors declare that they have no known competing financial interests or personal relationships that could have appeared to influence the work reported in this paper.

Acknowledgments

This work was supported by the National Natural Science Foundation of China (Grant number: 42101322), Fundamental Research Funds for the Central Universities (Grant number: 2024300388), Fundamental Research Funds for the Central Universities - Cemac “GeoX” Interdisciplinary Program (Grant number: 020714380210), and the Program for Outstanding Ph.D. Candidates of Nanjing University (Grant number: 202401A10). We are also grateful for the financial support provided by the National Youth Talent Support Program of China.

Appendix A. Supplementary data

Supplementary data to this article can be found online at <https://doi.org/10.1016/j.isprsjprs.2024.07.026>.

References

- Alkama, R., Cescatti, A., 2016. Biophysical climate impacts of recent changes in global forest cover. *Science* 351 (6273), 600–604. <https://doi.org/10.1126/science.aac8083>.
- Anderson, G.B., Bell, M.L., Peng, R.D., 2013. Methods to calculate the heat index as an exposure metric in environmental health research. *Environ. Health Perspect.* 121 (10), 1111–1119. <https://doi.org/10.1289/ehp.1206273>.
- Aparecido, L.M.T., Miller, G.R., Cahill, A.T., Moore, G.W., 2016. Comparison of tree transpiration under wet and dry canopy conditions in a Costa Rican premontane tropical forest. *Hydrol. Process.* 30 (26), 5000–5011. <https://doi.org/10.1002/hyp.10960>.
- Biardeau, L.T., Davis, L.W., Gertler, P., Wolfram, C., 2020. Heat exposure and global air conditioning. *Nat. Sustainability* 3 (1), 25–28. <https://doi.org/10.1038/s41893-019-0441-9>.
- Bowler, D.E., Buyung-Ali, L., Knight, T.M., Pullin, A.S., 2010. Urban greening to cool towns and cities: A systematic review of the empirical evidence. *Landsc. Urban Plan.* 97 (3), 147–155. <https://doi.org/10.1016/j.landurbplan.2010.05.006>.
- Chakraborty, T., Hsu, A., Manya, D., Sheriff, G., 2019. Disproportionately higher exposure to urban heat in lower-income neighborhoods: a multi-city perspective. *Environ. Res. Lett.* 14 (10), 105003 <https://doi.org/10.1088/1748-9326/ab3b99>.
- Cheng, X., Peng, J., Dong, J., Liu, Y., Wang, Y., 2022. Non-linear effects of meteorological variables on cooling efficiency of African urban trees. *Environ. Int.* 169, 107489 <https://doi.org/10.1016/j.envint.2022.107489>.
- Cheng, X., Liu, Y., Dong, J., Corcoran, J., Peng, J., 2023. Opposite climate impacts on urban green spaces’ cooling efficiency around their coverage change thresholds in major African cities. *Sustain. Cities Soc.* 88, 104254 <https://doi.org/10.1016/j.scs.2022.104254>.
- Du, M., Li, N., Hu, T., Yang, Q., Chakraborty, T.C., Venter, Z., Yao, R., 2024. Daytime cooling efficiencies of urban trees derived from land surface temperature are much higher than those for air temperature. *Environ. Res. Lett.* 19 (4), 044037 <https://doi.org/10.1088/1748-9326/ad30a3>.

- Falchetta, G., De Cian, E., Sue Wing, I., Carr, D., 2024. Global projections of heat exposure of older adults. *Nat. Commun.* 15 (1), 3678. <https://doi.org/10.1038/s41467-024-47197-5>.
- Hamada, S., Ohta, T., 2010. Seasonal variations in the cooling effect of urban green areas on surrounding urban areas. *Urban For. Urban Green.* 9 (1), 15–24. <https://doi.org/10.1016/j.ufug.2009.10.002>.
- Hsu, A., Sheriff, G., Chakraborty, T., Manya, D., 2021. Disproportionate exposure to urban heat island intensity across major US cities. *Nat. Commun.* 12 (1), 2721. <https://doi.org/10.1038/s41467-021-22799-5>.
- Huang, G., Zhou, W., Cadenasso, M.L., 2011. Is everyone hot in the city? Spatial pattern of land surface temperatures, land cover and neighborhood socioeconomic characteristics in Baltimore, MD. *Journal of Environmental Management* 92 (7), 1753–1759. <https://doi.org/10.1016/j.jenvman.2011.02.006>.
- Jungman, T., Cirach, M., Marando, F., Barboza, E.P., Khomenko, S., Masselot, P., Quijal-Zamorano, M., Mueller, N., Gasparrini, A., Urquiza, J., Heris, M., Thondoo, M., 2023. Cooling cities through urban green infrastructure: a health impact assessment of European cities. *Lancet* 401 (10376), 577–589. [https://doi.org/10.1016/S0140-6736\(22\)02585-5](https://doi.org/10.1016/S0140-6736(22)02585-5).
- Jenerette, G.D., Harlan, S.L., Buyantuev, A., Stefanov, W.L., Declet-Barreto, J., Ruddell, B.L., Myint, S.W., Kaplan, S., Li, X., 2016. Micro-scale urban surface temperatures are related to land-cover features and residential heat related health impacts in Phoenix, AZ USA. *Landscape Ecology* 31 (4), 745–760. <https://doi.org/10.1007/s10980-015-0284-3>.
- Jiao, M., Zhou, W., Zheng, Z., Wang, J., Qian, Y., 2017. Patch size of trees affects its cooling effectiveness: A perspective from shading and transpiration processes. *Agric. For. Meteorol.* 247, 293–299. <https://doi.org/10.1016/j.agrformet.2017.08.013>.
- Konarska, J., Uddling, J., Holmer, B., Lutz, M., Lindberg, F., Pleijel, H., Thorsson, S., 2016. Transpiration of urban trees and its cooling effect in a high latitude city. *Int. J. Biometeorol.* 60 (1), 159–172. <https://doi.org/10.1007/s00484-015-1014-x>.
- Laaidi, K., Zeghnoun, A., Dousset, B., Bretin, P., Vandoren, S., Giraudet, E., Beaudeau, P., 2012. The impact of heat islands on mortality in Paris during the August 2003 heat wave. *Environ. Health Perspect.* 120, 254–259. <https://doi.org/10.1289/ehp.1103532>.
- Lambers, H., Oliveira, R.S., 2019. Plant Water Relations. In: *Plant Physiological Ecology*. Springer, Cham. https://doi.org/10.1007/978-3-030-29639-1_5.
- Leng, S., Sun, R., Yan, M., Chen, L., 2024. Prevalent underestimation of tree cooling efficiency attributed to urban intrinsic heterogeneity. *Sustain. Cities Soc.* 105277. <https://doi.org/10.1016/j.scs.2024.105277>.
- Li, X., Gong, P., Zhou, Y., Wang, J., Bai, Y., Chen, B., Hu, T., Xiao, Y., Xu, B., Yang, J., Liu, X., 2020. Mapping global urban boundaries from the global impervious area (GAIA) data. *Environ. Res. Lett.* 15 (9), 094044. <https://doi.org/10.1088/1748-9326/ab9be3>.
- Li, Y., Zhao, M., Motesharrei, S., Mu, Q., Kalnay, E., Li, S., 2015. Local cooling and warming effects of forests based on satellite observations. *Nat. Commun.* 6 (1), 6603. <https://doi.org/10.1038/ncomms7603>.
- Li, M., Trugman, A.T., Peñuelas, J., Anderegg, W.R., 2024. Climate-driven disturbances amplify forest drought sensitivity. *Nat. Clim. Chang.* 1–7. <https://doi.org/10.1038/s41558-024-02022-1>.
- Luo, M., Lau, N.C., 2021. Increasing human-perceived heat stress risks exacerbated by urbanization in China: A comparative study based on multiple metrics. *Earth's Future* 9 (7). <https://doi.org/10.1029/2020EF001848> e2020EF001848.
- Massaro, E., Schifanella, R., Piccardo, M., Caporaso, L., Taubenböck, H., Cescatti, A., Duveiller, G., 2023. Spatially-optimized urban greening for reduction of population exposure to land surface temperature extremes. *Nat. Commun.* 14 (1), 2903. <https://doi.org/10.1038/s41467-023-38596-1>.
- Meehl, G.A., Tebaldi, C., 2004. More intense, more frequent, and longer lasting heat waves in the 21st century. *Science* 305 (5686), 994–997. <https://doi.org/10.1126/science.1098704>.
- Mitchell, D., 2021. Climate attribution of heat mortality. *Nat. Clim. Chang.* 11 (6), 467–468. <https://doi.org/10.1038/s41558-021-01049-y>.
- Mora, C., Dousset, B., Caldwell, I.R., Powell, F.E., Geronimo, R.C., Bielecki, C.R., Counsell, C.W., Dietrich, B.S., Johnston, E.T., Louis, L.V., Lucas, M.P., 2017. Global risk of deadly heat. *Nat. Clim. Chang.* 7 (7), 501–506. <https://doi.org/10.1038/nclimate3322>.
- Myint, S.W., Wentz, E.A., Brazel, A.J., Quattrochi, D.A., 2013. The impact of distinct anthropogenic and vegetation features on urban warming. *Landsc. Ecol.* 28 (5), 959–978. <https://doi.org/10.1007/s10980-013-9868-y>.
- Oke, T.R., Mills, G., Christen, A., Voogt, J.A., 2017. *Urban climates*. Cambridge University Press.
- Park, C.E., Jeong, S., Harrington, L.J., Lee, M.I., Zheng, C., 2020. Population ageing determines changes in heat vulnerability to future warming. *Environ. Res. Lett.* 15 (11), 114043. <https://doi.org/10.1088/1748-9326/abbd60>.
- Raymond, C., Matthews, T., Horton, R.M., 2020. The emergence of heat and humidity too severe for human tolerance. *Sci. Adv.* 6 (19), eaaw1838. <https://doi.org/10.1126/sciadv.aaw1838>.
- Rogan, J., Ziemer, M., Martin, D., Ratick, S., Cuba, N., DeLauer, V., 2013. The impact of tree cover loss on land surface temperature: A case study of central Massachusetts using Landsat Thematic Mapper thermal data. *Appl. Geogr.* 45, 49–57. <https://doi.org/10.1016/j.apgeog.2013.07.004>.
- Santamouris, M., 2014. Cooling the cities—a review of reflective and green roof mitigation technologies to fight heat island and improve comfort in urban environments. *Sol. Energy* 103, 682–703. <https://doi.org/10.1016/j.solener.2012.07.003>.
- Schwaab, J., Meier, R., Mussetti, G., Seneviratne, S., Bürgi, C., Davin, E.L., 2021. The role of urban trees in reducing land surface temperatures in European cities. *Nat. Commun.* 12 (1), 6763. <https://doi.org/10.1038/s41467-021-26768-w>.
- Sinha, P., Coville, R.C., Hirabayashi, S., Lim, B., Endreny, T.A., Nowak, D.J., 2021. Modeling lives saved from extreme heat by urban tree cover. *Ecol. Model.* 449, 109553. <https://doi.org/10.1016/j.ecolmodel.2021.109553>.
- Swann, A.L., Fung, I.Y., Chiang, J.C., 2012. Mid-latitude afforestation shifts general circulation and tropical precipitation. *Proceedings of the National Academy of Sciences* 109 (3), 712–716. <https://doi.org/10.1073/pnas.1116706108>.
- Tayyebi, A., Jenerette, G.D., 2016. Increases in the climate change adaption effectiveness and availability of vegetation across a coastal to desert climate gradient in metropolitan Los Angeles, CA, USA. *Sci. Total Environ.* 548, 60–71. <https://doi.org/10.1016/j.scitotenv.2016.01.049>.
- Tuholske, C., Caylor, K., Funk, C., Verdin, A., Sweeney, S., Grace, K., Peterson, P., Evans, T., 2021. Global urban population exposure to extreme heat. *Proc. Natl. Acad. Sci.* 118 (41). <https://doi.org/10.1073/pnas.2024792118> e2024792118.
- United Nations, Department of Economic and Social Affairs, Population Division. (2022). Probabilistic population projections, Rev. 1 based on the World Population Prospects 2019, Rev. 1. <http://population.un.org/wpp>.
- Wang, C., Wang, Z.H., Wang, C., Myint, S.W., 2019a. Environmental cooling provided by urban trees under extreme heat and cold waves in US cities. *Remote Sens. Environ.* 227, 28–43. <https://doi.org/10.1016/j.rse.2019.03.024>.
- Wang, C., Liu, Z., Du, H., Zhan, W., 2023. Regulation of urban morphology on thermal environment across global cities. *Sustain. Cities Soc.* 97, 104749. <https://doi.org/10.1016/j.scs.2023.104749>.
- Wang, Y., Wang, A., Zhai, J., Tao, H., Jiang, T., Su, B., Yang, J., Wang, G., Liu, Q., Gao, C., Fischer, T., 2019b. Tens of thousands additional deaths annually in cities of China between 1.5 °C and 2.0 °C warming. *Nat. Commun.* 10 (1), 3376. <https://doi.org/10.1038/s41467-019-11283-w>.
- Wang, J., Zhou, W., Jiao, M., Zheng, Z., Ren, T., Zhang, Q., 2020. Significant effects of ecological context on urban trees' cooling efficiency. *ISPRS J. Photogramm. Remote Sens.* 159, 78–89. <https://doi.org/10.1016/j.isprsjprs.2019.11.001>.
- Wang, J., Zhou, W., Jiao, M., 2022. Location matters: planting urban trees in the right places improves cooling. *Front. Ecol. Environ.* 20 (3), 147–151. <https://doi.org/10.1002/fee.2455>.
- Wang, J., Zhou, W., 2022. More urban greenspace, lower temperature? Moving beyond net change in greenspace. *Agric. For. Meteorol.* 322, 109021. <https://doi.org/10.1016/j.agrformet.2022.109021>.
- Yang, Q., Huang, X., Tong, X., Xiao, C., Yang, J., Liu, Y., Cao, Y., 2022. Global assessment of urban trees' cooling efficiency based on satellite observations. *Environ. Res. Lett.* 17 (3), 034029. <https://doi.org/10.1088/1748-9326/ac4c1c>.
- Yin, Y., He, L., Wennberg, P.O., Frankenberg, C., 2023. Unequal exposure to heatwaves in Los Angeles: Impact of uneven green spaces. *Sci. Adv.* 9 (17), eade8501. <https://doi.org/10.1126/sciadv.ade8501>.
- Yu, Z., Xu, S., Zhang, Y., Jørgensen, G., Vejre, H., 2018. Strong contributions of local background climate to the cooling effect of urban green vegetation. *Sci. Rep.* 8 (1), 6798. <https://doi.org/10.1038/s41598-018-25290-w>.
- Yuan, B., Zhou, L., Hu, F., Zhang, Q., 2022. Diurnal dynamics of heat exposure in Xi'an: A perspective from local climate zone. *Build. Environ.* 222, 109400. <https://doi.org/10.1016/j.buildenv.2022.109400>.
- Zhao, L., Oleson, K., Bou-Zeid, E., Kravchenko, E.S., Bray, A., Zhu, Q., Zheng, Z., Chen, C., Oppenheimer, M., 2021. Global multi-model projections of local urban climates. *Nat. Clim. Chang.* 11 (2), 152–157. <https://doi.org/10.1038/s41558-020-00958-8>.
- Zhao, J., Zhao, X., Wu, D., Meili, N., Fatichi, S., 2023. Satellite-based evidence highlights a considerable increase of urban tree cooling benefits from 2000 to 2015. *Glob. Chang. Biol.* 29 (11), 3085–3097. <https://doi.org/10.1111/gcb.16667>.
- Zhou, W., Wang, J., Cadenasso, M.L., 2017. Effects of the spatial configuration of trees on urban heat mitigation: A comparative study. *Remote Sens. Environ.* 195, 1–12. <https://doi.org/10.1016/j.rse.2017.03.043>.
- Zhou, W., Huang, G., Pickett, S.T., Wang, J., Cadenasso, M.L., McPhearson, T., Grove, J. M., Wang, J., 2021. Urban tree canopy has greater cooling effects in socially vulnerable communities in the US. *One Earth* 4 (12), 1764–1775. <https://doi.org/10.1016/j.oneear.2021.11.010>.